

A Leaky Wave Antenna With Dielectric Superstrate on Perforated Dielectric Spacer

Takuya Kaji¹, Hiroyasu Sato¹, *Member, IEEE*, Qiang Chen², *Senior Member, IEEE*, Shimpei Nagae, Akira Kumagai, and Osamu Kagaya³, *Member, IEEE*

Abstract—In this article, a leaky wave antenna with dielectric superstrate (LWADS) on the perforated dielectric spacer is proposed. The LWADS has an asymmetric structure with a half-filled dielectric spacer and with a nonfilled spacer to make a quasi-cutoff region. The half-filled dielectric spacer is periodically perforated, and the beam direction of the leaky wave is controlled by changing the hole radius. In general, the unwanted radiation occurs in the broadside direction when the beam of the leaky wave is tilted at a large angle, and this unwanted radiation is avoided by providing these perforated dielectric spacers. The proposed design is validated by measurements at X-band, and it is shown that a high gain tilted beam pattern with peak gains of 14 dBi is obtained not only at $\theta = 20^\circ$ and 40° but also at the wide-angle of $\theta = 60^\circ$. Since the effective permittivity can be controlled by the hole radius, an array of LWADS with different beam angles can be realized with the same height and a multibeam antenna with switched feeding can be realized.

Index Terms—Dielectric antennas, gain measurement, glass, leaky waves, multibeam antennas.

I. INTRODUCTION

NEXT-GENERATION mobile communications are expected to use high-frequency bands such as millimeter wave and terahertz bands. These high-frequency bands have high straightness and high propagation loss, which limit the coverage area of a single base station. Therefore, a dense arrangement of base stations and beamforming technology to generate a sharp beam in a desired direction is required [1], [2]. Phased array antennas are commonly used as a technique to realize beamforming, but the transmission line losses to feed a large number of antenna elements are not ignorable, and the digital phase shifters used to control the phase of each element are expensive [3], [4]. For those reasons, multibeam switching antennas with multiple antennas having different beam directions are expected [5], [6], [7], [8]. In addition, in urban areas surrounded by tall buildings, there

are many obstructions, and the radio wave weakens rapidly in the shadowing region of buildings. To compensate for these problems, the antennas used in the construction of small cells, where base stations are densely installed, are located on the rooftops and walls of buildings and it is not easy to add more antennas due to restrictions on installation locations and the cityscape. Therefore, antennas with low loss and flexible installation are expected as base station antennas in urban areas for next-generation mobile communications.

A leaky wave antenna with dielectric superstrate (LWADS) has been studied as a method to obtain a high-gain pencil beam [9], [10], [11], [12], [13]. LWADS has the advantage of simple construction, low profile, and high gain with only a single feed. LWADS can also produce conical beams by changing the height and thickness of the dielectric superstrate. If this conical beam can be converted into a tilted beam with a single radiation direction, it is effective as a multiantenna with different beam directions as expected [14], [15], [16].

Several methods have been proposed to transform this conical beam into a high-gain tilted beam [14], [15], [16]. In [14] and [15], feeding elements are placed at the edges of the LWADS to achieve 45° and 23° tilted beams. In [16], an array antenna consisting of eight patch antennas was used as a feeding element, and the beam direction by the array is aligned to realize a tilted beam of 30° , however, there is no wide-angle beam of 60° or more. In [17], it was shown that the unwanted broadside radiation mode can be suppressed by increasing the relative permittivity of the dielectric spacer to the value larger than 1.33 but it is not applied to the one-directional tilted beam.

In general, different tilt angles can be obtained by changing the height of the dielectric spacer, which makes the configuration of a multibeam antenna system with different height antennas. This problem can be solved by sandwiching dielectrics with different relative permittivities, as shown in Fig. 1(a). This asymmetric structure allows the radio waves fed from the center to propagate toward both right and left sides with different phase constants, forming dual tilted beams with different angles. However, it is difficult to obtain a dielectric material with the desired permittivity. As one of the approaches to solve this problem, the perforated dielectric using a large number of air holes with diameters sufficiently smaller than the wavelength is applicable to control the effective permittivity [18], [19], [20], [21], [22]. Recently, applications of perforated dielectric materials for the control

Manuscript received 29 September 2022; revised 3 March 2023; accepted 27 March 2023. Date of publication 14 April 2023; date of current version 2 June 2023. (Corresponding author: Hiroyasu Sato.)

Takuya Kaji, Hiroyasu Sato, and Qiang Chen are with the Department of Communications Engineering, Graduate School of Engineering, Tohoku University, Sendai, Miyagi 980-8579, Japan (e-mail: takuya.kaji.t2@dc.tohoku.ac.jp; hiroyasu.sato.b1@tohoku.ac.jp; qiang.chen.a5@tohoku.ac.jp).

Shimpei Nagae, Akira Kumagai, and Osamu Kagaya are with AGC Inc., Marunouchi, Tokyo 100-8405, Japan (e-mail: shimpei.l.nagae@agc.com; akira.kumagai@agc.com; osamu.kagaya@agc.com).

Color versions of one or more figures in this article are available at <https://doi.org/10.1109/TAP.2023.3266036>.

Digital Object Identifier 10.1109/TAP.2023.3266036

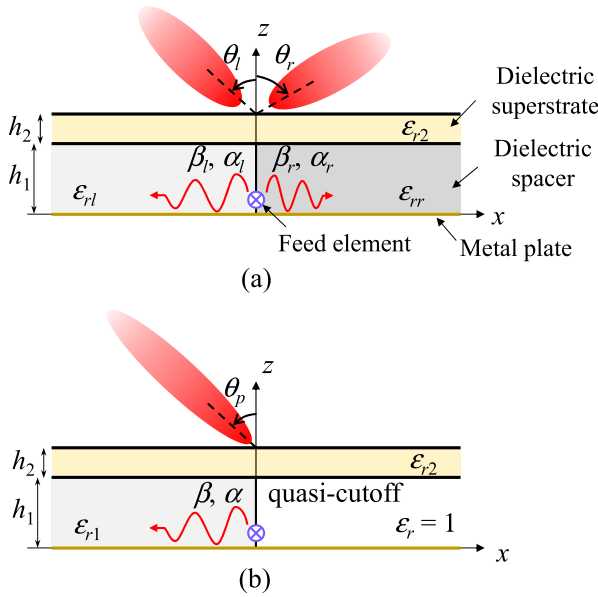


Fig. 1. Geometry of the LWADS with dielectric superstrate on the asymmetric dielectric spacer. (a) Two different dielectric spacers with different permittivities ($\epsilon_{r2} > \epsilon_{r1}$). (b) Dielectric spacer with the truncated right half region.

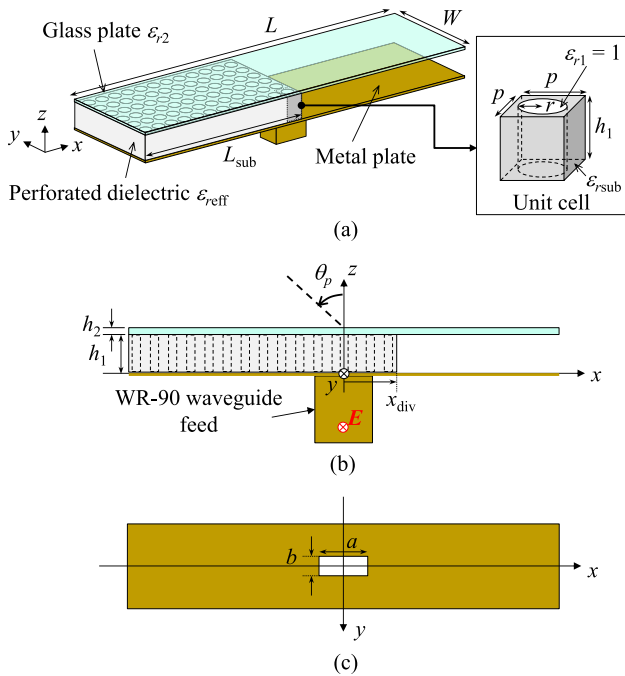


Fig. 2. Structure of LWADS partially filled with perforated dielectric fed by a rectangular waveguide. (a) Perspective view. (b) Side view. (c) Bottom view.

of effective permittivity have been employed in antennas such as the dielectric resonator antennas [23], [24], the reflectarrays [25], [26], and the lens antennas [27], [28], and they have been recognized as effective solutions to achieve desired permittivities.

In this article, an LWADS with an asymmetric structure in which a dielectric spacer with periodic holes is proposed, and a part of the dielectric spacer is truncated, as shown in Fig. 2(a). By properly designing the thickness of dielectric spacer h_1 , the

quasi-cutoff region in which no leaky-wave modes generated is formed in the air region of the truncated side, and leaky waves are generated only in the region of perforated dielectric exists. The effect of this quasi-cutoff region, in which the fields attenuate rapidly toward the opposite of the desired direction, allows the generation of a tilted beam directed only toward the desired direction. The angle of tilted beams can be controlled at a fixed frequency by changing the hole radius of the perforated dielectric spacer. Furthermore, by designing the effective relative permittivity of the perforated dielectric with a value larger than 1.33, and by combining the technique of quasi-cutoff region described above, unwanted radiation toward the broadside direction can be suppressed, enabling wide-angle tilted beams with high gain characteristics.

This article is composed of sections shown below. The design of LWADS with perforated dielectric and tilted beam design is discussed in Section II, experimental and simulation results are presented in Section III, and conclusions are shown in Section IV.

II. ANTENNA DESIGN

A. Design of LWADS With Perforated Dielectric Spacer

First, consider the LWADS, where the dielectric spacer is full-filled with dielectric materials with thickness and relative permittivity of (h_1, ϵ_{r1}) and with (h_2, ϵ_{r2}) in the dielectric superstrate, respectively. In this case, the optimum thickness of each layer to obtain maximum gain toward the desired beam direction θ_p is generally provided by [9], [10], [11], [12], and [13] as

$$h_1 = \frac{m\lambda_0}{2} \frac{1}{\sqrt{\epsilon_{r1} - \sin^2 \theta_p}} \quad (1)$$

$$h_2 = \frac{(2n-1)\lambda_0}{4} \frac{1}{\sqrt{\epsilon_{r2} - \sin^2 \theta_p}} \quad (2)$$

where λ_0 is the wavelength in free space, and m and n are positive integers. In the case when $\theta_p = 0^\circ$, both the phase constant and attenuation constant of the leaky wave decrease, and a pencil beam toward the broadside will be radiated. In the case when $\theta_p > 0^\circ$, the phase constant of the leaky wave increases, and the conical tilted beam will be radiated.

It is known that the directivity gain G_d of LWADS increases proportional to the ratio of the relative permittivity of the dielectric superstrate to that of the dielectric spacer in the case of an infinite structure, as shown in the following [9]:

$$G_d \propto \frac{\epsilon_{r2}}{\epsilon_{r1}}. \quad (3)$$

Therefore, it is effective to use a dielectric slab with high permittivity ϵ_{r2} for the superstrate, and the spacer layer should be filled with air as $\epsilon_{r1} = 1$. The perforated dielectric having an effective relative permittivity ϵ_{reff} is adopted in the dielectric spacer. The structure of the proposed LWADS is shown in Fig. 2. The propagation constant of the leaky wave in the xy plane is controlled by changing the air holes of a perforated dielectric with air holes penetrating in z -direction. Perforated dielectrics are generally introduced by drilling holes

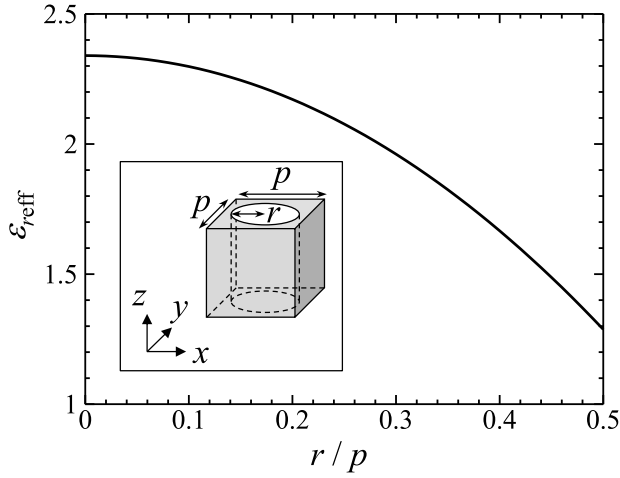


Fig. 3. Effective relative permittivity ϵ_{reff} of unit-cell as a function of r/p .

with various sizes. Considering the periodic perforation of circular holes in dielectric materials, each unit cell forms a cuboid with dimensions of $p \times p \times h_1$, and a cylindrical structure with a radius of r with a center axis along the thickness direction of dielectric material. When the relative permittivity of the perforated area is denoted as ϵ_{ra} and the rest is ϵ_{rb} , ϵ_{reff} can generally be approximated by the volume ratio of the two media under the condition $p < \lambda_0/2$ [20] as

$$\epsilon_{\text{reff}} = \frac{(\pi r^2 h_1) \epsilon_{ra} + (p^2 h_1 - \pi r^2 h_1) \epsilon_{rb}}{p^2 h_1}. \quad (4)$$

Substituting $\epsilon_{ra} = 1$ and $\epsilon_{rb} = \epsilon_{\text{rsub}}$, we obtain

$$\epsilon_{\text{reff}} = \epsilon_{\text{rsub}} + (1 - \epsilon_{\text{rsub}}) \frac{\pi r^2}{p^2}. \quad (5)$$

Note that ϵ_{rsub} represents the relative permittivity of the material used for the perforated dielectric itself. An example of the calculation by (5) is shown in Fig. 3. Since the range of r is $0 \leq r \leq p/2$, the range of ϵ_{reff} becomes

$$\epsilon_{\text{rsub}} + (1 - \epsilon_{\text{rsub}}) \frac{\pi}{4} \leq \epsilon_{\text{reff}} \leq \epsilon_{\text{rsub}}. \quad (6)$$

In this article, the high-density polyethylene (HDPE) was selected as the material for the perforated dielectric spacer due to its excellent mechanical and electrical properties [29]. When $\epsilon_{\text{rsub}} = 2.34$, the range of ϵ_{reff} is $1.29 \leq \epsilon_{\text{reff}} \leq 2.34$.

The above approach using perforated dielectrics with inhomogeneous structure is useful to control dielectric permittivity, however, the hole has a cylindrical geometry and waves in this structure will be totally different from those in the case of homogeneous dielectric materials. This inhomogeneous structure will limit the frequency range and the anisotropy of permittivity will appear. From the viewpoint that the propagation direction of leaky waves is limited in the xy plane, the effect of anisotropy will not be received remarkably. In addition, as discussed in [17], unwanted radiation appears when $\epsilon_{r1} \leq 1.33$ are selected, resulting in a reduction of directive gain, however, once a larger ϵ_{r1} is selected, it results in a lower gain as shown in (3). Therefore, the thickness and relative permittivity of the dielectric spacer should be set

TABLE I
PARAMETERS OF THE PERFORATED DIELECTRIC SPACERS

θ_p	ϵ_{r1}	r
20°	1.56	4.31 mm
40°	1.85	3.40 mm
60°	2.19	1.89 mm

TABLE II
PARAMETERS USED FOR THE SIMULATION

Parameter	Value	Parameter	Value
L	240 mm	a	22.9 mm
L_{sub}	120 mm	b	10.2 mm
W	240 mm	ϵ_{r1}	1.85
h_1	12.5 mm	ϵ_{r2}	6.8
h_2	3 mm	x_{div}	0 mm

appropriately and the use of the perforated dielectrics is the desirable solution.

In this article, the tilted beams with three different angles in a range from $\theta_p = 20^\circ$ to $\theta_p = 60^\circ$ with 20° increments were demonstrated. Applying (6) to (1), the range of h_1 is

$$\begin{aligned} \frac{m\lambda_0}{2} \frac{1}{\sqrt{\epsilon_{\text{rsub}} - \sin^2 \theta_p}} &\leq h_1 \\ &\leq \frac{m\lambda_0}{2} \frac{1}{\sqrt{\epsilon_{\text{rsub}} + (1 - \epsilon_{\text{rsub}}) \frac{\pi}{4} - \sin^2 \theta_p}} \end{aligned} \quad (7)$$

where left and right terms of (7) are corresponding to cases of $r/p = 0$ and $r/p = 0.5$. Note that (7) is valid when h_2 satisfies (2), because (1) and (2) are not independent. In the case when $f = 10$ GHz, $\epsilon_{\text{rsub}} = 2.34$, and $m = 1$, the range of h_1 is provided by $11.9 \text{ mm} \leq h_1 \leq 13.9 \text{ mm}$ to realize all desired tilt angles θ_p in a range from 20° to 60° . h_1 can be selected as 11.9 mm to realize the lowest relative permittivity of the perforated dielectric spacer in order to maximize the gain. However, the selection of $r/p = 0.5$ causes a problem in manufacturing that each unit cell cannot be connected to each other, and therefore, $r/p = 0.46$ was selected which corresponds to $h_1 = 12.5$ mm. Setting $p = 10$ mm, r is determined for each angle of the tilted beam, and they are shown in Table I.

As the dielectric superstrate, we chose soda lime glass, which is widely used as window glass, and the relative permittivity of glass was assumed to be $\epsilon_{r2} = 6.8$ [30]. The dielectric superstrate thickness h_2 satisfying (2) is $h_2 = 2.90$, 2.97 , and 3.05 mm when $\theta_p = 20^\circ$, 40° , and 60° , respectively. $h_2 = 3$ mm was selected as an approximation of those values and as the available glass plates.

B. Quasi-Cutoff Region for Tilted Beam

In order to evaluate the propagation constant of leaky waves in a half-filled dielectric spacer, FDTD analysis of infinite leaky waveguide in case of $h_1 = 12.5$ mm was performed as shown in Fig. 4. SEMCAD X [31] was used for the simulations. All simulations were performed lossless. The parameters of the analysis model are shown in Table II. A dielectric

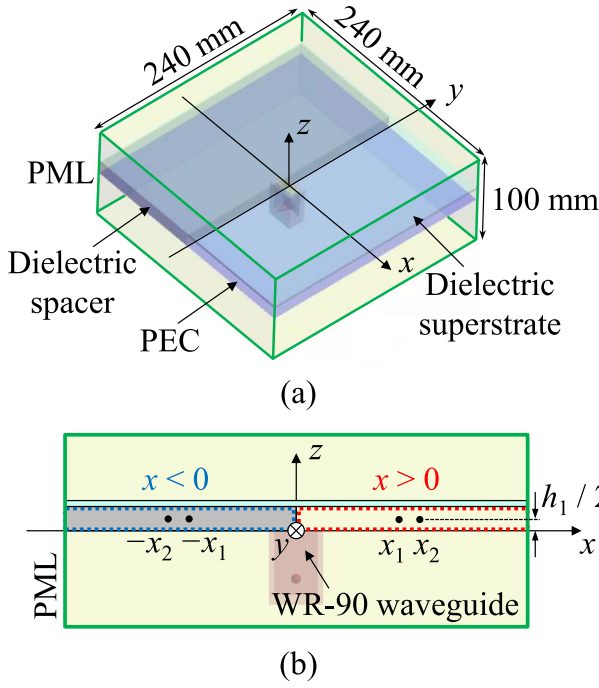


Fig. 4. Analysis model for the SEMCAD X simulation. (a) Perspective view. (b) Side view. PEC: perfect electric conductor.

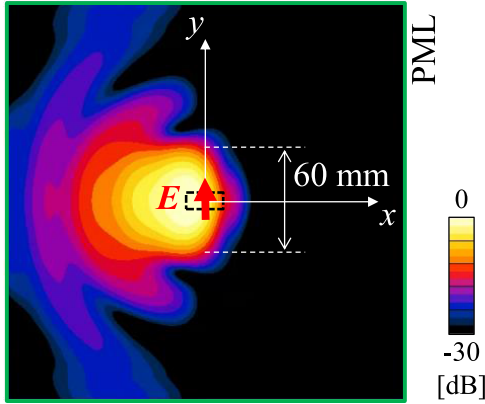


Fig. 5. Simulated normalized aperture $|E_y|$ -field distribution at 10 GHz.

spacer exists only in a region of $x < 0$. A y -polarized feeding waveguide was located at the center of the ground plane. The leaky waveguide is terminated by the perfect matched layer (PML) in order to eliminate the reflection at the terminal, and only the traveling wave propagates in the leaky waveguide. By calculating time domain response $E_x(t, x = x_1, y = 0, z = h_1/2)$ and $E_x(t, x = x_2, y = 0, z = h_1/2)$, the phase constant and the attenuation constant can be calculated by

$$\alpha + j\beta = \frac{1}{x_2 - x_1} \left\{ \frac{\mathcal{F}[E_x(t, x = x_2, y = 0, z = h_1/2)]}{\mathcal{F}[E_x(t, x = x_1, y = 0, z = h_1/2)]} \right\} \quad (8)$$

where \mathcal{F} denotes the Fourier transform.

Fig. 5 shows the aperture E_y field distribution on the xy plane, 5 mm away from the surface ($z = 20.5$ mm) of the dielectric superstrate. It is observed a quite weak field

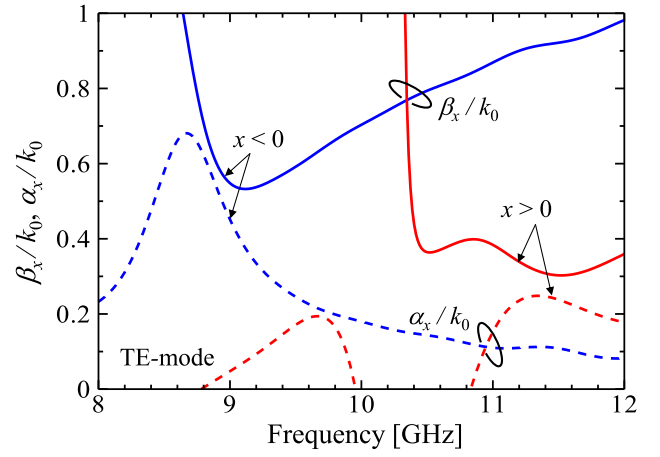


Fig. 6. Normalized phase constant and attenuation constant in the region of $x > 0$ and $x < 0$.

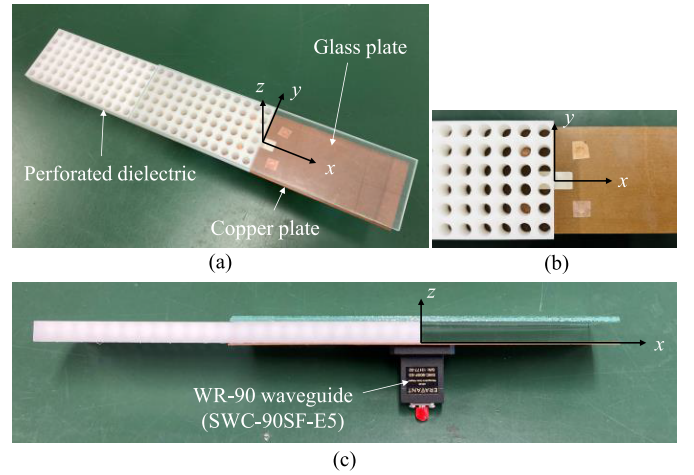


Fig. 7. Photograph of the fabricated prototype of the proposed LWADS. (a) Perspective view. (b) Top view (without glass plate). (c) Side view.

in the region of $x > 0$ corresponding quasi-cutoff regions. Furthermore, the spread of the electric field in the y -direction is limited near the waveguide feeding aperture in a range of 60 mm. Therefore, a narrow-width structure can be realized.

The results of the phase constant and attenuation constant are shown in Fig. 6. Phase constant toward $-x$ -direction of $\beta/k_0 = 0.703$ at 10 GHz is observed which corresponds to the radiation of leaky wave as $\sin\theta_p = \beta/k_0$, $\theta_p = 44.7^\circ$ which almost agrees with the desired angle of $\theta_p = 40^\circ$. In contrast, the phase constant toward $+x$ -direction diverges at 10 GHz, and mode is not observed, and we call the region of $x > 0$ as “quasi-cutoff region.” Thus, the air region was described as a quasi-cutoff and numerically demonstrated in the simulation.

III. MEASUREMENT RESULTS

A photograph of the prototype of LWADS is shown in Fig. 7(a). The parameters of LWADS are shown in Table III. The dielectric superstrate is made of 3.3-mm-thick soda glass plates with a thickness of $h_2 = 3.3$ mm. HDPE with a thickness of $h_1 = 12.5$ mm was used for the perforated dielectrics. Three types of perforated dielectric with hole sizes

TABLE III
GEOMETRICAL PARAMETERS OF THE PROPOSED LWADS PROTOTYPE

Parameter	Value	Parameter	Value
L	240 mm	b	10.2 mm
L_{sub}	240 mm	ϵ_{sub}	2.34
W	60 mm	ϵ_2	6.8
h_1	12.5 mm	p	10 mm
h_2	3.3 mm	r	Variable
a	22.9 mm	x_{div}	Variable

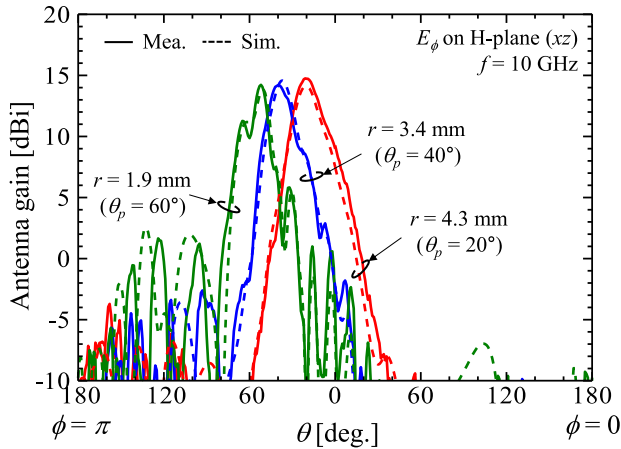


Fig. 8. Measured and simulated antenna gain pattern of LWADS with half-filled perforated dielectric.

TABLE IV
MEASURED RESULTS

Parameter		Measured value at 10 GHz (E_ϕ on H-plane)	
θ_p	r	θ_{max}	G_{max}
20°	4.31 mm	21° ($\phi = \pi$)	14.8 dBi
40°	3.40 mm	40° ($\phi = \pi$)	14.2 dBi
60°	1.89 mm	52° ($\phi = \pi$)	14.2 dBi

corresponding to each θ_p were fabricated. Each length of the perforated dielectric was $L_{\text{sub}} = 240$ mm. Fig. 7(c) shows the case when the half of length of 120 mm was inserted between a ground plane and a dielectric soda glass superstrate, however, the length provided by $L_{\text{sub}}/2 + x_{\text{div}}$ was inserted in order to evaluate the effect of the x -coordinate of the right edge of perforated dielectric x_{div} . A copper plate was used as the ground plane, and a standard WR-90 waveguide (SWC-90SF-E5) was connected at the center of the copper plate.

Radiation patterns were measured in an anechoic chamber. Fig. 8 shows the measured and simulated antenna gain patterns in the H-plane of the three types of LWADS with changing hole radius r . Almost good agreement between the measured and simulated results was observed. Table IV shows the measured antenna gains of these three types. It is observed that tilted beam angles of $\theta = 21^\circ$, 40° , and 52° are obtained in the cases of $r = 4.3$, 3.4 , and 1.9 mm, respectively, those values are almost the same as the desired beam directions. It is noted that a tilted beam is generated only on the $\phi = \pi$ side, and an antenna gain of over 14 dBi was observed. In the case of $r = 1.9$ mm, the beam is slightly distorted, however,

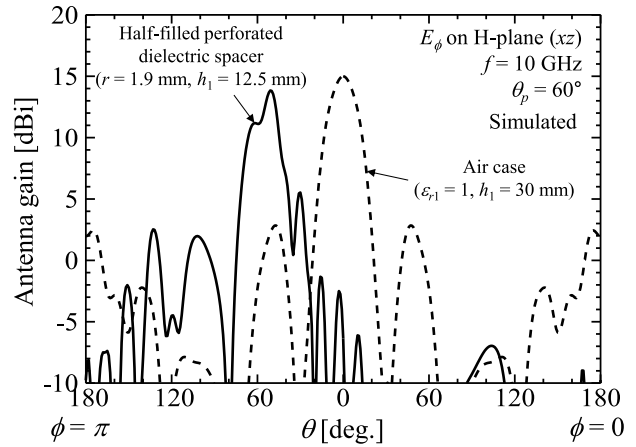


Fig. 9. Simulated antenna gain pattern in the case with the half-filled perforated dielectric spacer ($r = 1.9$ mm and $h_1 = 12.5$ mm) and the air case ($\epsilon_{r1} = 1$ and $h_1 = 30$ mm).

the gain of 14 dBi is maintained. A small dip around 63° is observed, however, it is clarified by a simulation that this dip can be eliminated by cutting the redundant section of the dielectric spacer in a range of $-240 \text{ mm} \leq x \leq -120 \text{ mm}$. It can be considered that the effective aperture of LWADS becomes small as θ_p increases; however, the decrease of the gain is not so large. This effect can be explained that the attenuation constant provided by $\alpha = k (\epsilon_{\text{reff}} - \sin^2 \theta_p)^{3/2} \cot \theta_p$ (k : constant) [11] becomes small as θ_p increases which correspond to the fact that the excited area of the leaky wave with small attenuation increases as θ_p increases.

Fig. 9 shows the simulated antenna gain pattern in the case with the half-filled perforated dielectric and the nonfilled case ($\epsilon_{r1} = 1$). Note that both cases were designed to obtain a large, tilted beam of $\theta_p = 60^\circ$. In the case of air, dual beams with a beam direction of 47° which is far from 60° were observed and the unwanted broadside radiation has appeared. However, this unwanted radiation disappeared in the presence of the perforated dielectric, and wide-angle tilted beam became possible by the same height LWADS.

Fig. 10 shows the simulated results of the 3-D radiation pattern of LWADS with the dimension of Table III. It is observed that the beam is not a general fan beam but has directivity in the azimuthal direction.

Fig. 11 shows the frequency characteristics of the antenna gain pattern of the three different types of LWADS in the cases of $r = 4.3$, 3.4 , and 1.9 mm in the frequency range of 8–12 GHz. As shown in Fig. 11(a)–(c), a tilted beam is observed from 8 to 11 GHz. In the frequency range of $f > 11$ GHz, the additional beam is observed in the $\phi = 0$ side corresponding to the leaky waves excited in the air region ($x > 0$).

Finally, the effect of the position x_{div} on the antenna gain was investigated. x_{div} was swept from -15 to 15 mm in 5 mm increments. Fig. 12 shows the antenna gain in the H-plane at $\theta = 40^\circ$ in the $\phi = \pi$ side as a function of x_{div} . The antenna gain reaches a maximum of 14.3 dBi when $x_{\text{div}} = 5$ mm. In the case when $|x_{\text{div}}| \leq 5$ mm, the change of the gain is within 1 dB, while the gain decreases over 3 dB

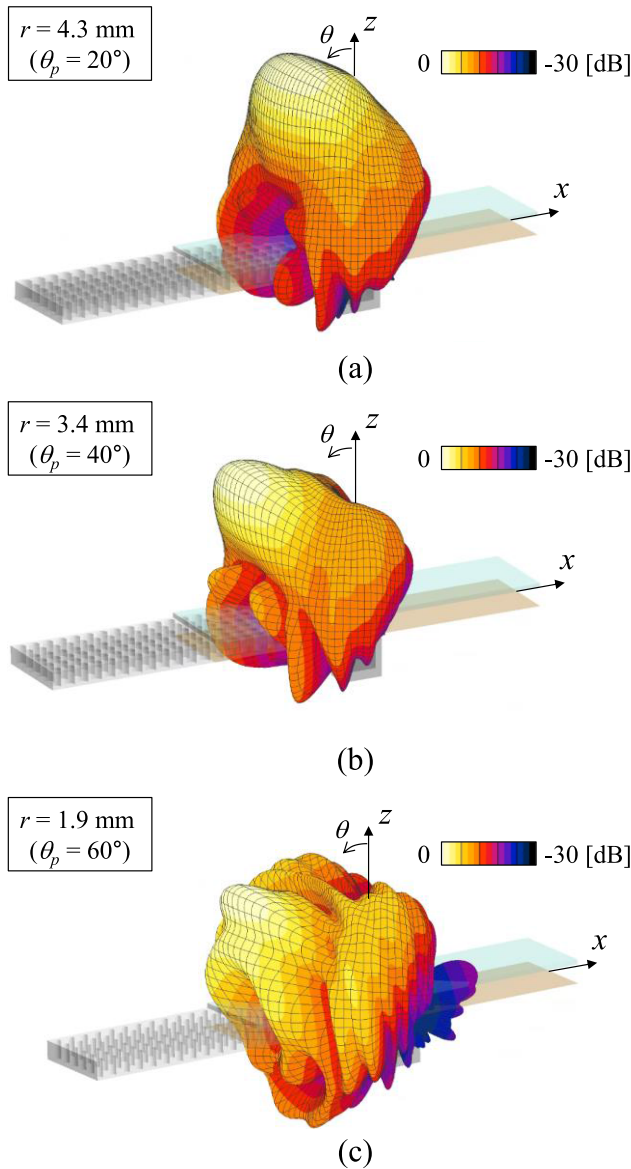


Fig. 10. Simulated 3-D radiation patterns of the three types of LWADS at 10 GHz. (a) $r = 4.3$ mm ($\theta_p = 20^\circ$). (b) $r = 3.4$ mm ($\theta_p = 40^\circ$). (c) $r = 1.9$ mm ($\theta_p = 60^\circ$). Other parameters are shown in Table III ($x_{\text{div}} = 0$ mm).

from the maximum value in the case when $|x_{\text{div}}| \geq 10$ mm. Fig. 13 shows the antenna gain pattern in H-plane at 10 GHz when $x_{\text{div}} = -10, 0$, and 10 mm. The case of $x_{\text{div}} = 0$ mm corresponds to the configuration when half of the waveguide aperture is covered by the perforated dielectric. In the cases of $x_{\text{div}} = -10$ and 10 mm, the distorted beam pattern is observed. However, those distortion disappeared in the case of $x_{\text{div}} = 0$ mm. It is considered that around $x_{\text{div}} = 0\text{--}5$ mm is the optimal value to convert the waveguide mode to the leaky wave mode sufficiently. Why this configuration of $x_{\text{div}} = 0$ mm works well is not clarified sufficiently. Therefore, it will be necessary to investigate the feeding structure suitable for the excitation of leaky wave mode in the perforated dielectric.

A comparison table with the previous works of the LWADS which can generate one-directional tilted beams is summarized in Table V. Note that previous works have not achieved

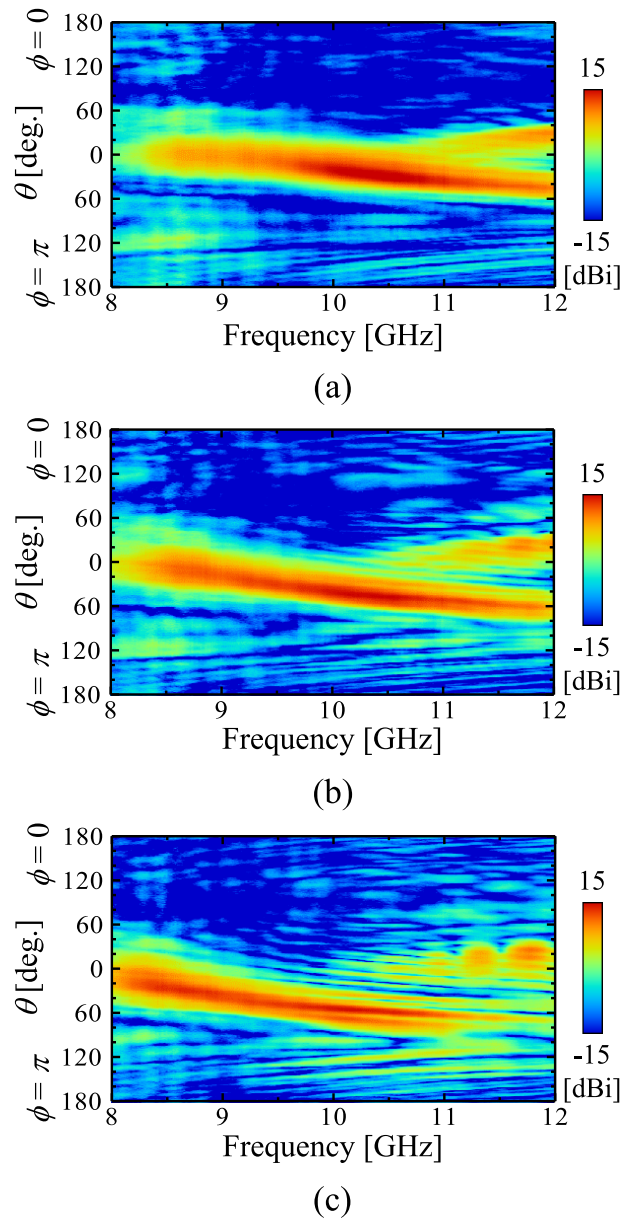


Fig. 11. Measured antenna gain of the three types of LWADS [E_ϕ on H-plane (xz)]. (a) $r = 4.3$ mm ($\theta_p = 20^\circ$). (b) $r = 3.4$ mm ($\theta_p = 40^\circ$). (c) $r = 1.9$ mm ($\theta_p = 60^\circ$). Other parameters are shown in Table III ($x_{\text{div}} = 0$ mm).

TABLE V
COMPARISON WITH THE PREVIOUS WORKS

Ref.	Scan angle	Antenna gain [dBi]	Permittivity of dielectric superstrate	Aperture size	Feed type
[14]	45°	18.2	10.8	$11\lambda_0 \times \text{NA}$	Monopole antenna
[15]	23°	16.19	10.2	$13\lambda_0 \times 17\lambda_0$	Waveguide Patch antenna array
[16]	30°	23	6 (multi-superstrates)	NA	Waveguide
This work	52°	14.2	6.8	$8\lambda_0 \times 2\lambda_0$	Waveguide

wide-angle beams. In this article, it is achieved the wide-angle beam by controlling the permittivity of the dielectric spacer and by forming the quasi-cutoff region. Furthermore, the

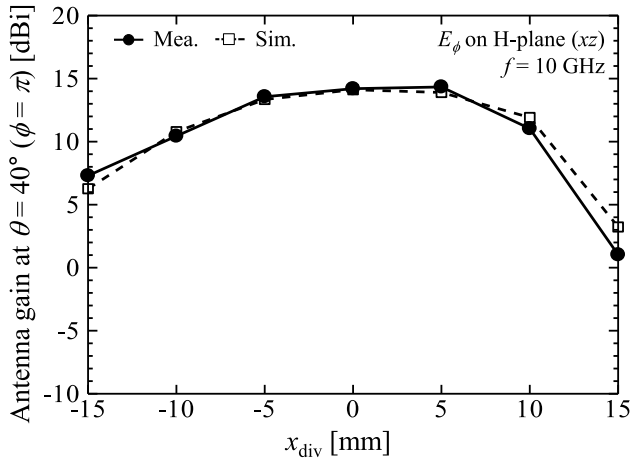


Fig. 12. Measured and simulated antenna gain at $\theta = 40^\circ$ in the $\phi = \pi$ side as a function of x_{div} .

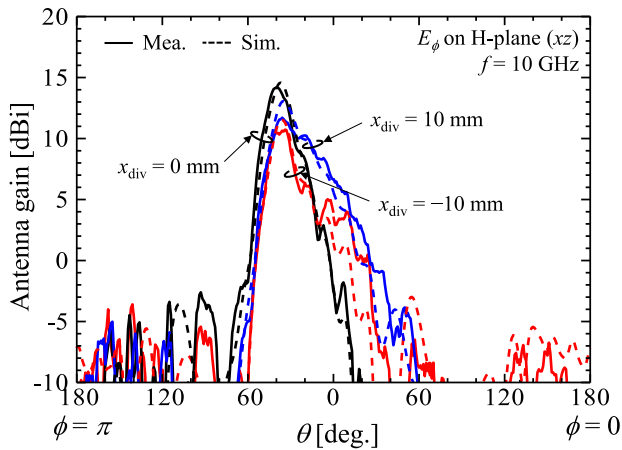


Fig. 13. Measured and simulated antenna gain pattern in H-plane of LWADS partially filled with perforated dielectric with different x_{div} .

proposed antennas are with a reduced width compared with previous LWADS. The region of $-240 \text{ mm} \leq x \leq -120 \text{ mm}$ is the redundant area, and the region of $-120 \text{ mm} \leq x \leq 0 \text{ mm}$ is the effective area. On the other hand, the region of $0 \text{ mm} \leq x \leq 120 \text{ mm}$ is the evanescent region for quasi-cutoff. Since the gain of the leaky wave, the traveling-wave antenna depends on the antenna length and the extension of length in the $-x$ -direction will improve the gain. Of course, the aperture efficiency of the antenna in Fig. 7 is small compared with the case without the evanescent region; however, this region works well to decrease the unwanted opposite radiation. As far as we know, the proposed antenna is the most promising candidate for applications that can be mounted on flat glass and directed to a wide angle.

IV. CONCLUSION

In this article, an LWADS on the perforated dielectric has been proposed and the wide-angle tilted beam was experimentally demonstrated. The LWADS has an asymmetric structure with a half-filled dielectric spacer and with a nonfilled spacer to make a quasi-cutoff region. It was experimentally shown that the beam direction of $\theta = 21^\circ$, 40° , and 52° with high gain

of over 14 dBi was realized with different hole radii of 4.3, 3.4, and 1.9 mm, respectively, with the same height. It is also demonstrated that the half-filled perforated dielectric works to reduce the unwanted broadside radiation which appears when the tilted angle of the beam increases. The LWADS will be extended to realize the multibeam-switching antenna array.

REFERENCES

- [1] T. S. Rappaport et al., "Millimeter wave mobile communications for 5G cellular: It will work!" *IEEE Access*, vol. 1, pp. 335–349, 2013.
- [2] F. Boccardi, R. W. Heath, A. Lozano, T. L. Marzetta, and P. Popovski, "Five disruptive technology directions for 5G," *IEEE Commun. Mag.*, vol. 52, no. 2, pp. 74–80, Feb. 2014.
- [3] E. Levine, G. Malamud, S. Shtrikman, and D. Treves, "A study of microstrip array antennas with the feed network," *IEEE Trans. Antennas Propag.*, vol. 37, no. 4, pp. 426–434, Apr. 1989.
- [4] M. Khalili, R. Tafazolli, T. A. Rahman, and M. R. Kamarudin, "Design of phased arrays of series-fed patch antennas with reduced number of the controllers for 28-GHz mm-Wave applications," *IEEE Antennas Wireless Propag. Lett.*, vol. 15, pp. 1305–1308, 2015.
- [5] H. Tanabe, K. Sakakibara, and N. Kikuma, "Multibeam-switching millimeter-wave antenna using beam-tilting design in perpendicular plane to feeding line of microstrip comb-line antenna," in *IEEE MTT-S Int. Microw. Symp. Dig.*, Mar. 2017, pp. 139–142.
- [6] S. Liu and Q. Chen, "Dual-beam gain-reconfigurable antennas using a shared reflectarray aperture," in *Proc. Int. Symp. Antennas Propag. (ISAP)*, 2019, pp. 1–3.
- [7] C. Di Paola, S. Zhang, K. Zhao, Z. Ying, T. Bolin, and G. F. Pedersen, "Wideband beam-switchable 28 GHz quasi-Yagi array for mobile devices," *IEEE Trans. Antennas Propag.*, vol. 67, no. 11, pp. 6870–6882, Nov. 2019.
- [8] A. J. Pascual et al., "An antenna array for photonic beam switching in mm-Wave wireless communications," in *Proc. 15th Eur. Conf. Antennas Propag. (EuCAP)*, Mar. 2021, pp. 1–4.
- [9] D. Jackson and N. Alexopoulos, "Gain enhancement methods for printed circuit antennas," *IEEE Trans. Antennas Propag.*, vol. AP-33, no. 9, pp. 976–987, Sep. 1985.
- [10] H. Yang and N. Alexopoulos, "Gain enhancement methods for printed circuit antennas through multiple superstrates," *IEEE Trans. Antennas Propag.*, vol. AP-35, no. 7, pp. 860–863, Jul. 1987.
- [11] D. R. Jackson and A. A. Oliner, "A leaky-wave analysis of the high-gain printed antenna configuration," *IEEE Trans. Antennas Propag.*, vol. AP-36, no. 7, pp. 905–910, Jul. 1988.
- [12] R. Aoki, H. Sato, and K. Sawaya, "Fundamental study of high gain EBG resonator antenna," (in Japanese), *IEICE Tech. Rep.*, vol. 104, no. 209, pp. 103–108, Jul. 2004.
- [13] D. R. Jackson et al., "The fundamental physics of directive beaming at microwave and optical frequencies and the role of leaky waves," *Proc. IEEE*, vol. 99, no. 10, pp. 1780–1805, Oct. 2011.
- [14] E. Schmidhammer, J. Detlefsen, and H. Ostner, "Influence of a 45° corner-reflector on the radiation pattern of a planar leaky-wave antenna," in *Proc. IEEE Antennas Propag. Soc. Int. Symp. Dig.*, Jul. 1996, pp. 2016–2019.
- [15] F. Scatone, M. Ettore, B. Eddo, R. Sauleau, and N. J. G. Fonseca, "Truncated leaky-wave antenna with cosecant-squared radiation pattern," *IEEE Antennas Wireless Propag. Lett.*, vol. 17, no. 5, pp. 841–844, May 2018.
- [16] L. Leger, T. Monediere, E. Arnaud, and B. Jecko, "Multisources and beam steered EBG antennas," in *Proc. 11th Int. Symp. Antenna Technol. Appl. Electromagn.*, Jun. 2005, pp. 1–4.
- [17] T. Zhao, D. R. Jackson, J. T. Williams, H. Y. D. Yang, and A. A. Oliner, "2-D periodic leaky-wave antennas—Part I: Metal patch design," *IEEE Trans. Antennas Propag.*, vol. 53, no. 11, pp. 3505–3514, Nov. 2005.
- [18] T. Morita and S. B. Cohn, "Microwave lens matching by simulated quarter-wave transformers," *IRE Trans. Antennas Propag.*, vol. 4, no. 1, pp. 33–39, 1956.
- [19] P. S. Kildal, K. Jakobsen, and K. S. Rao, "Meniscuslens-corrected corrugated horn: A compact feed for a Cassegrain antenna," *IEE Proc.*, vol. 131, no. 6, pp. 390–394, Dec. 1984.
- [20] J. B. Muldavin and G. M. Rebeiz, "Millimeter-wave tapered-slot antennas on synthesized low permittivity substrates," *IEEE Trans. Antennas Propag.*, vol. 47, no. 8, pp. 1276–1280, Aug. 1999.

- [21] W. Shao, H. Sato, X. Li, K. K. Mutai, and Q. Chen, "Perforated extensible 3-D hyperbolic secant lens antenna for directive antenna applications using additive manufacturing," *Opt. Exp.*, vol. 29, no. 12, pp. 18932–18949, Jun. 2021.
- [22] W. Shao and Q. Chen, "2-D beam-steerable generalized Mikaelian lens with unique flat-shape characteristic," *IEEE Antennas Wireless Propag. Lett.*, vol. 20, no. 10, pp. 2033–2037, Oct. 2021.
- [23] I. A. Zubir et al., "A low-profile hybrid multi-permittivity dielectric resonator antenna with perforated structure for Ku and K band applications," *IEEE Access*, vol. 8, pp. 151219–151228, 2020.
- [24] C. Tong, H. I. Kremer, N. Yang, and K. W. Leung, "Compact wideband circularly polarized dielectric resonator antenna with dielectric vias," *IEEE Antennas Wireless Propag. Lett.*, vol. 21, no. 6, pp. 1100–1104, Jun. 2022.
- [25] M. Abd-Elhady, W. Hong, and Y. Zhang, "A Ka-band reflectarray implemented with a single-layer perforated dielectric substrate," *IEEE Antennas Wireless Propag. Lett.*, vol. 11, pp. 600–603, 2012.
- [26] Y. He, Z. Gao, D. Jia, W. Zhang, B. Du, and Z. N. Chen, "Dielectric metamaterial-based impedance-matched elements for broadband reflectarray," *IEEE Trans. Antennas Propag.*, vol. 65, no. 12, pp. 7019–7028, Dec. 2017.
- [27] A.-E. Mahmoud, W. Hong, Y. Zhang, and A. Kishk, "W-band multilayer perforated dielectric substrate lens," *IEEE Antennas Wireless Propag. Lett.*, vol. 13, pp. 734–737, 2014.
- [28] M. K. T. Al-Nuaimi and W. Hong, "Discrete dielectric reflectarray and lens for E-band with different feed," *IEEE Antennas Wireless Propag. Lett.*, vol. 13, pp. 947–950, 2014.
- [29] K. Seeger, "Microwave measurement of the dielectric constant of high-density polyethylene," *IEEE Trans. Microw. Theory Techn.*, vol. 39, no. 2, pp. 352–354, Feb. 1991.
- [30] G. I. Kiani, A. Karlsson, L. Olsson, and K. P. Esselle, "Glass characterization for designing frequency selective surfaces to improve transmission through energy saving glass windows," in *Proc. Asia-Pacific Microw. Conf.*, Dec. 2007, pp. 1–4.
- [31] *SEMCAD X by SPEAG*. Accessed: Apr. 1, 2022. [Online]. Available: <https://www.speag.com>



Takuya Kaji received the B.E. degree from Tohoku University, Sendai, Japan, in 2021, where he is currently pursuing the M.E. degree.

His current research interests include glass antennas.



Hiroyasu Sato (Member, IEEE) received the B.E. and M.E. degrees from Chuo University, Tokyo, Japan, in 1993 and 1995, respectively, and the D.E. degree from Tohoku University, Sendai, Japan, in 1998.

He is currently an Assistant Professor with the Department of Communications Engineering, Tohoku University. His current research interests include the experimental study of electromagnetic waves, computational electromagnetics, antennas in plasma, antennas for plasma production, broad-

band antennas, wireless power transfer, and active/passive millimeter wave imaging.

Dr. Sato is a member of the Institute of Electronics, Information and Communication Engineers (IEICE). He received the first place in the Best Paper Award from the International Symposium on Antennas and Propagation (ISAP) in 2017.



Qiang Chen (Senior Member, IEEE) received the B.E. degree from Xidian University, Xi'an, China, in 1986, and the M.E. and D.E. degrees from Tohoku University, Sendai, Japan, in 1991 and 1994, respectively.

He is currently a Chair Professor with the Electromagnetic Engineering Laboratory, Department of Communications Engineering, Faculty of Engineering, Tohoku University. His primary research interests include antennas, microwave and millimeter waves, electromagnetics measurements, and computational electromagnetics.

Dr. Chen is a Fellow of the Institute of Electronics, Information and Communication Engineers (IEICE). He received the Best Paper Award and the Zenichi Kiyasu Award from IEICE, in 2009. He served as the Chair for IEICE Technical Committee on Photonics-Applied Electromagnetics Measurement from 2012 to 2014, the IEICE Technical Committee on Wireless Power Transfer from 2016 to 2018, and the IEEE Antennas and Propagation Society Tokyo Chapter from 2017 to 2018. He is currently the Chair of the IEICE Technical Committee on Antennas and Propagation.



Shimpei Nagae received the B.E. and M.E. degrees from Tohoku University, Sendai, Japan, in 2018 and 2020, respectively.

He joined AGC Inc., Tokyo, Japan, in 2020. Since 2020, he has been engaged in research on glass antennas.



Akira Kumagai received the B.Sc. and M.Sc. degrees from Tohoku University, Sendai, Japan, in 2008 and 2010, respectively.

In 2010, he joined Tokyo Keiki Inc., Tokyo, Japan. In 2019, he joined AGC Inc., Yokohama, Japan, where he is engaged in research and development on antennas for radio communication systems.



Osamu Kagaya (Member, IEEE) received the B.S., M.E., and D.E. degrees in engineering from the Tokyo University of Agriculture and Technology (TUAT), Tokyo, Japan, in 1999, 2001, and 2022, respectively.

He joined AGC Inc., Yokohama, Japan, in 2001. Since 2001, he has been engaged in research on glass antennas and electromagnetic scattering.